Monograph:

Owens, D.H. and Chotai, A. (1981) Robust Controller Design for Uncertain Dynamic Systems Using Approximate Models. Research Report. ACSE Report 161 PT 1 . Department of Control Engineering, University of Sheffield, Mappin Street, Sheffield

ROBUST CONTROLLER DESIGN FOR UNCERTAIN DYNAMIC SYSTEMS USING APPROXIMATE MODELS

PART I: THE SINGLE-INPUT/SINGLE-OUTPUT CASE

by

D.H.Owens B.Sc., A.R.C.S., Ph.D., A.F.I.M.A., C.Eng., M.I.E.E.

and

A.Chotai B.Sc., Ph.D.

Department of Control Engineering,
University of Sheffield,
Mappin Street, Sheffield S1 3JD.

Research Report No. 161

October 1981

This work is supported by the Science and Engineering Research Council under Grant GR/B/23250.

Indexing Terms: Controller design; process control; stability; stability theory; robustness; approximation; sampled-data systems; digital control; nonlinear systems.

Abstract

Controller design for continuous and discrete systems whose models are unknown or highly complex are frequently based upon the use of a simple, approximate and, very often, rough-and-ready model. In such circumstances it is vital to be able to quantify the degree of uncertainty to be expected from the use of such a model for prediction of closed-loop characteristics. It is shown how classical frequency-domain design techniques can be extended to incorporate information deduced from the observed differences between open-loop plant and approximate model step response to quantify this uncertainty and, in particular, to guarantee closed-loop stability and tracking of step demands. A modification of this analysis also yields the possibility of bounding the error in prediction of closed-loop transient performance. The approaches are all graphical in nature and could be easily implemented in an interactive computer-aided-design mode.

1. Introduction

The use of approximate plant models is an everyday fact of life in control systems design. They arise in several different ways such as

(a) the explicit use of model reduction techniques applied to a known but possibly large-scale plant model,

(b) the explicit use of curve-fitting or identification procedures applied to transient data obtained from plant trials or simulation of a complex plant model, or

(c) the implicit use of conceptual models that underly commonly used on-lining tuning methods such as that due to Ziegler and Nichols.

In all cases controller design decisions are made on the basis of the expected behaviour of the approximate model in the closed-loop situation. Clearly, the techniques can be highly successful in predicting closed-loop performance of the real plant if the approximate model chosen is fairly accurate. If, however the chosen model is significantly inaccurate then care must be exercised in interpreting theoretical predictions! Although accurate models can be used with confidence, they tend to have fairly high dynamic order and hence can introduce computational and interpretive problems, particularly in non-specialist hands. In contrast, rough-and-ready models tend to be low order and lead to rapid 'pencil and paper' designs to form the basis for further, perhaps on-line, investigations. The deliberate use of approximate models can produce direct benefits therefore, but efforts must be made to cope with the observed errors. The empirical technique of designing to ensure adequate gain and phase margins provides a qualitative frequency domain solution to cope with the problem of modelling errors but it would clearly be of great value to be able to assess the effect of these errors in a more precise manner, particulary if the revised design procedure uses only simple open-loop plant data such as step response characteristics and has a simple graphical interpretation that relates closely to well-known classical design techniques. This problem is the subject of this paper and its companion. The work represents a substantial generalization of the technique described in ref. (2). This paper restricts its attention to single-input/single-output systems. The multivariable case with its extra problems and possibilities is left to the companion paper[1].

The paper logically divides into several sections. In section 2 we provide a frequency domain technique for the design of robust control systems for uncertain dynamic systems using approximate models. In essence this section provides a graphical means of coping with observed differences in performance between plant and model by 'smudging' of the standard inverse Nyquist plot commonly used in system design. Section 3 invokes some elementary techniques from functional analysis to point out that, under certain conditions that are easily checked in practice, closed-loop stability can be assessed by visual inspection of the transient performance of the approximating feedback system and carries the bonus that numerical bounds on the deterioration in predicted transient performance can be obtained even in the presence of measurement nonlinearities. In section 4, the generalization of these ideas to discrete/sampled-data plant is outlined.

2. Frequency Domain Design based on Approximate Models

The problem considered here is the design of the proper, rational forward path controller K in Fig. 1(a) for the plant G in the presence of the proper, rational measurement dynamics F. All elements are assumed to be continuous and linear and it is assumed that the detailed dynamics of the plant are either unknown or regarded as unnecessarily or inconveniently complex for the design exercise under consideration. It is supposed however, that the response Y(t) of the plant from zero initial conditions to a unit step input at t = o can be estimated from plant trials or simulation of an available complex model. The response Y(t) will, in practice, contain errors but, for the purposes of this paper, these will be assumed to be small enough to be negligible.

Given the data Y(t) suppose now that an approximate model G_A of the real plant G is constructed by fitting to the transient data Y or by model reduction. The response $Y_A(t)$ of G_A from zero initial conditions to a unit step input at t = o can be obtained by simulation. The control system K can now be designed, by any means at the designers disposal, to ensure the required stability and transient performance from the approximating feedback system of Fig. 1(b). The problem considered in this section is how the observed open-loop error

$$E(t) = Y(t) - Y_A(t) \qquad (1)$$

between step responses of the real and approximate plant can be used during the design exercise to simultaneously ensure the stability of the real configuration Fig. 1(a).

Note that we do not necessarily assume that G and G_A are represented by rational transfer functions but we do require that, assuming zero initial conditions, they can be described by linear input-output maps of convolution form(19)

$$y(t) = \int_o^t h(t')u(t-t')dt' \ , \ y_A(t) = \int_o^t h_A(t')u_A(t-t')dt' \qquad (2)$$

where $h \in L_1(o,+\infty)$ and $h_A \in L_1(o,+\infty)$ have well-defined Laplace transforms (and are usually piecewise continuous) and the modelling error is stable in the sense that

$$\int_o^\infty |h(t) - h_A(t)|dt < +\infty \qquad (3)$$

This form of model allows the possibility, for example, of time-delays in the system.

Finally, note the obvious relations

$$Y(t) = \int_o^t h(t')dt' \ , \ Y_A(t) = \int_o^t h_A(t')dt' \quad , \ t \geq 0 \qquad (4)$$

and deduce that the signal $Y - Y_A$ is stable as, using (3) and (4),

$$|Y(t) - Y_A(t)| \leq \int_o^t |h(t') - h_A(t')|dt'$$

$$\leq \int_o^\infty |h(t') - h_A(t')|dt'$$

$$< +\infty \quad , \forall \ t \geq o \qquad (5)$$

2.1 Frequency Domain Stability Theory

Suppose that the controller K has been successfully designed to stabilize the approximate model G_A in the configuration of Fig. 1(b). This condition can be represented by the return-difference relationship[19]

$$\inf_{\text{Re } s \geq o} |1 + G_A(s)K(s)F(s)| > 0 \qquad (6)$$

If the same controller K is hooked up to the real plant in the configuration of Fig. 1(a) then stability will be assured only if the similar relation

$$\inf_{\text{Re } s \geq o} |1 + G(s)K(s)F(s)| > 0 \qquad (7)$$

is satisfied.

These relations are most usefully combined by writing

$$(1+GKF) = (1+G_AKF)(1 + (1+G_AKF)^{-1}KF(G-G_A)) \qquad (8)$$

when (7) can be replaced by the sufficient condition

$$\inf_{\text{Re } s \geq o} | 1 + (1+G_AKF)^{-1}KF(G-G_A)| > 0 \qquad (9)$$

Given the assumed uncertainty about the real plant G, the authors know of no way that this relationship can be used in design. It is however, possible to replace it by a slightly conservative, but more easily checked (see Theorem 1), condition based on the result:

Lemma 1: If the chosen controller K stabilizes the approximate model G_A in the configuration of Fig. 1(b), then it will also stabilize the real uncertain plant G in the configuration of Fig. 1(a) if

(a) the composite system GKF is both controllable and observable, and

(b) $\lambda_1 \cdot \lambda_2 < 1$ (10)

where, if D is the usual Nyquist contour in the complex plane,

$$\lambda_1 \triangleq \sup_{s \in D} \left| (1 + G_A(s)K(s)F(s))^{-1} K(s)F(s) \right| \tag{11}$$

and λ_2 is any known upper bound for

$$\lambda_3 \triangleq \sup_{\text{Re } s \geq 0} \left| G(s) - G_A(s) \right| \tag{12}$$

Proof: Condition (a) guarantees the absence of hidden modes in the system and hence that asymptotic stability is implied by input/output stability. Next note that

$$\inf_{\text{Re } s \geq 0} \left| 1 + (1 + G_A KF)^{-1} KF (G - G_A) \right|$$

$$\geq 1 - \sup_{\text{Re } s \geq 0} \left| (1 + G_A KF)^{-1} KF \right| \sup_{\text{Re } s \geq 0} \left| G - G_A \right|$$

$$\geq 1 - \lambda_1 \lambda_3 \tag{13}$$

The stability assumption ensures that $(1+G_A KF)^{-1} KF$ is analytic in the interior of D and hence achieves its maximum modulus on the boundary. The result follows as (10) implies (9) by (13).

2.2 Frequency Response Bounds from Transient Data

The clear problem with direct application of lemma 1 is that, although λ_1 can be computed in terms of known quantities, λ_2 could, on the surface, present a problem. If, however, the error (eqn. (1)) between open-loop step responses is known, it is possible to bound λ_3 in terms of the graphical procedure implicit in the following simple result:

Proposition 1: If $g \in L_1(o,+\infty)$, d is a real scalar and

$$f(t) \triangleq d + \int_o^t g(t')dt' \tag{14}$$

is bounded and continuous on the infinite open interval $o < t < +\infty$ with local maxima or minima at times $t_1 < t_2 < \ldots\ldots$ satisfying $\sup t_j = +\infty$ in the extended half-line $t > o$, then, taking $t_o = 0$, we have, for any $T \geqslant 0$,

$$|d| + \int_o^T |g(t)|dt = N_T(f) \tag{15}$$

where the functional

$$N_T(f) \triangleq |f(o+)| + \sum_{k=1}^{k^*(T)} |f(t_k) - f(t_{k-1})| + |f(T) - f(t_{k^*})|$$

$$N_\infty(f) \triangleq \sup_{T \geqslant o} N_T(f) \tag{16}$$

(with $k^*(T)$ equal to the largest integer k such that $t_k < T$) is simply the norm of f regarded as a function of bounded variation[3] on the half-open interval $o < t \leqslant T$.

(Note: for each fixed f, $N_T(f)$ is clearly a monotonically increasing function of T).

<u>Proof</u>: Using (14) it is easily seen that the local maxima and minima of f correspond to 'cross-over points' of g. This is illustrated in some detail in Fig. 2(a) and (b) for the case of a finite number of stationary points in $[0,\infty)$. Note that $t = +\infty$ is a stationary point in our definition in this case. The case of an infinite number of stationary points is illustrated in Fig. 2(c). Note that $t = +\infty$ is not a stationary point in this case. In both cases write

$$|d| + \int_0^T |g(t)|dt$$

$$= |d| + \sum_{k=1}^{k^*(T)} \int_{t_{k-1}}^{t_k} |g(t)|dt + \int_{t_k^*}^{T} |g(t)|dt \tag{17}$$

and note that the sign-definiteness of g on each subinterval ensures that

$$\int_{t_{k-1}}^{t_k} |g(t)|\, dt = \left| \int_{t_{k-1}}^{t_k} g(t)\, dt \right| \tag{18}$$

The result follows as $f(0+) = d$ and, for $k \geq 1$,

$$\int_{t_{k-1}}^{t_k} g(t)dt = f(t_k) - f(t_{k-1}) \tag{19}$$

As an immediate corrollary to this result, we can state the following lemma which provides an explicit technique for computing a bound λ_2 by inspection of $E(t)$.

<u>Lemma 2</u>: If the plant modelling error is stable in the sense of (3), then

$$\sup_{\text{Re } s\geq 0} |G(s)-G_A(s)| = \lambda_3 \leq \lambda_2 \triangleq N_\infty(E) = \sum_{k\geq 1} |E(t_k)-E(t_{k-1})| \tag{20}$$

is a convenient upper bound on the modelling error $G - G_A$.
(Note: $t_0 = 0$ and $t_1 < t_2 < \ldots$ are points where the transient error $E(t)$ achieves local maxima or minima in the extended half-line $t > 0$).

Proof: Simply note that

$$G(s) - G_A(s) = \int_o^{\infty} e^{-st}(h(t) - h_A(t)dt \tag{21}$$

and that, for Re s $\geqslant$ o,

$$\left| \int_o^{\infty} e^{-st}(h(t) - h_A(t))dt \right| \leqslant \int_o^{\infty} \left| h(t) - h_A(t) \right| dt \tag{22}$$

The result follows by applying Proposition 1 to

$$E(t) = \int_o^{t} (h(t') - h_A(t')dt' \tag{23}$$

noting that E(o+) = O.

2.3 A Graphical Stability Criterion for Uncertain Systems

A condition of lemma 1 and 2 yields a powerful and easily applied graphical stability criterion as follows:

Theorem 1: If the controller K stabilizes the approximate model G_A in the configuration of Fig. 1(b), then it will also stabilize the real uncertain plant G in the configuration of Fig. 1(a) if,

(a) The plant modelling error is stable in the sense of equation (3),

(b) The composite system GKF is both controllable and observable,

(c) the inequality

$$N_{\infty}(E) \limsup_{\substack{|s| \to \infty \\ \mathrm{Re}\, s \geqslant o}} \left| \frac{K(s)F(s)}{1+G_A(s)K(s)F(s)} \right| < 1 \tag{24}$$

is satisfied, and

(d) the 'confidence band' generated by plotting the inverse Nyquist locus of $G_A(s)K(s)F(s)$ for $s = i\,\omega$, $\omega \geqslant o$ with superimposed 'confidence circles' at each point of radius

$$r(i\omega) \triangleq N_\infty(E) \; |G_A^{-1}(i\omega)| \tag{25}$$

does not contain or touch the (-1,o) point of the complex plane. (Note: see Fig. 3 for a graphical illustration of condition (d), noting that the radii of the confidence circles are proportional to the chosen modelling error and are zero if the plant model is exact).

Proof: Using (a) and (b), lemmas 1 and 2 indicate that stability will be achieved if

$$\sup_{s \in D} \left| \frac{K(s)F(s)}{1 + K(s)F(s)G_A(s)} \right| \; N_\infty(E) < 1 \tag{26}$$

Consideration of the 'infinite semi-circular' part of D yields (c). The imaginary axis then reduces (26) to the requirement that, for $-\infty < \omega < \infty$,

$$\left| 1 + (G_A(i\omega)K(i\omega)F(i\omega))^{-1} \right| > N_\infty(E) \; |G_A^{-1}(i\omega)| \tag{27}$$

which is simply (d) as the contribution from the negative imaginary axis is just the complex conjugate of that from the positive imaginary axis. The theorem is hence proved.

The application of the result proceeds by verification of the conditions of the theorem and could proceed as follows:

Step 1: Obtain the plant response Y(t) from zero initial conditions to a unit step input.

Step 2: Choose an approximate plant model G_A with the property that the modelling error $G - G_A$ is stable. If the plant G is stable this reduces to ensuring that G_A is stable. If the plant G is unstable then G_A must contain the 'unstable part' of G(see ref.(2)). Calculate $Y_A(t)$, E(t) and hence $N_\infty(E)$.

Step 3: Design the controller K(s) for $G_A(s)$ to obtain the required stability and performance characteristics from the approximating feedback system of Fig. 1(b). This design can proceed by any means available but can be guided by (c) as (24) implicitly puts a preliminary bound on the control gain allowed. The use of the inverse Nyquist locus of G_A KF as the basis of the design of K may be particularly useful in the light of step 4.

Step 4: Plot the inverse Nyquist locus of $G_A(s)K(s)F(s)$ for $s = i\omega$, $\omega \geq 0$, and superimpose confidence circles at sufficiently many frequency points to enable the form of the confidence band to be deduced. If the (-1,0) lies inside or on the boundary of the band return to Step 3. Otherwise the design is successful if the problem of Step 5 is soluble.

Step 5: Check that GKF is both controllable and observable. As pointed out in ref. (2), this type of problem does require some structural information concerning the plant G. For example, if $F(s) \equiv 1$, K(s) is a proportional plus integral controller and the plant is described by a rational transfer function G(s), it reduces to the requirement that G(s) is both controllable and observable and has no zero at the origin of the complex plane. This can be checked if the plant is stable by checking that $\lim_{t\to+\infty} Y(t) \neq 0$.

2.4 A Note on the Calculation of N(E)

The application of the above technique relies on accurate calculation of $N_\infty(E)$ given the (assumed accurate) step response Y(t). The two particular sources of error that will naturally arise in practice are due to (i) the general fact that the error E(t) is only available on a finite time-interval $0 \leq t \leq T$ and (ii) inevitable errors creep in due to difficulties in estimating the times $t_k, k \geq 1$, due to, for example, the use of sampled response data where t_k could be in error by up to the sample interval. These general problems are considered in Appendix 9 and lead to the general inclusion that they will be negligible if the data length T is long enough and the time errors/sampling rate are small enough/fast enough.

2.5 An Illustrative Example

To illustrate the application of the above theory in an elementary but representative situation suppose that the uncertain plant has an unknown model given by the transfer function

$$G(s) = \frac{1}{(s+1)^3} \tag{28}$$

and hence that the plant step response $Y(t)$ given by

$$Y(t) = 1 - (1 + t + \tfrac{1}{2} t^2)e^{-t} \tag{29}$$

is known in graphical form as illustrated in Fig. 4(a). Suppose that we choose the approximate model described by the transfer function

$$G_A(s) = \frac{1}{(s+1)^2} \tag{30}$$

we can easily verify that its step response

$$Y_A(t) = 1 - (1+t)e^{-t} \tag{31}$$

takes the form indicated in Fig. 4(a) and that the error $E(t) = Y(t)-Y_A(t)$ is stable (indicating that $G - G_A$ is stable) of the form

$$E(t) = -\tfrac{1}{2} t^2 e^{-t} \tag{32}$$

illustrated in Fig. 4(b). Note that it is not monotonic and hence that previous results[2] do not apply in this case. The required parameter ($N_\infty(E)$ is obtained by the graphical procedure described in Proposition 1 with the data $t_o = 0$, $t_1 = 2$, $t_2 = +\infty$ i.e.

$$N_\infty(E) = 4\,e^{-2} = 0.54 \tag{33}$$

The next step is the choice of unity feedback controller K for G_A. Our ultimate aim is to obtain a proportional plus integral controller

$$K(s) = K_1 + \frac{K_2}{s} \quad , K_1 > 0 \, , K_2 \geqslant 0 \tag{34}$$

but initially we will take the case of proportional control $K_2 = 0$. A preliminary bound on K_1 is obtained from (24) i.e.

$$N_\infty(E) \lim_{|s| \to \infty} \left| \frac{K}{1 + KG_A} \right| = N_\infty(E) \; |K_1| < 1 \tag{35}$$

or, using (33),

$$|K_1| < 1.85 \tag{36}$$

(Note: this bound is to be compared with the real stability range $0 \leqslant K_1 < 8$ for G. There is clearly some pessimism in the result but this is to be expected as the modelling error E(t) is not small. We can only remove this pessimism by improving the model G_A!). Our detailed choice of K_1 could proceed by choosing it to produce a damping of $1/\sqrt{2}$ in the approximating feedback system i.e. choose $K_1 = 1.0$. This certainly satisfies (36) and the inverse Nyquist plot of $G_A K F = G_A$ with superimposed confidence circles shown in Fig. 5 indicates that the (-1,0) point does not lie in or on the confidence band. In fact, conditions (a), (c) and (d) of theorem 1 are satisfied and we can conclude that the uncertain plant (28) will be stable under unity feedback with gain $K_1 = 1$ provided that GKF = G (i.e. the plant) is both controllable and observable.

The inclusion of integral action can proceed in a similar manner with condition (24) again leading to the fundamental constraint (36) on proportional gain. Again choosing $K_1 = 1.0$, we will also choose $K_2 = 0.4$ to ensure the stabilization of the approximate model with reset time $K_1/K_2=2.5$. The relevant inverse Nyquist locus with confidence band is given in Fig. 6. Conditions (a), (c) and (d) of theorem 1 are clearly satisfied and hence the designed controller will stabilize the uncertain plant if GKF = GK is both controllable and observable. This will be almost surely satisfied if G is controllable and observable as the only other source of problems could be a zero of G at s = o or a pole of G at s = -0.4. Examination of Y(t) indicates that G has no zero at s=o.

Finally, for comparative purposes, the closed-loop responses of real and approximating feedback systems from zero initial conditions to a unit step demand are shown in Fig. 7. Note that the responses have similar overall dynamic characteristics and identical steady-states.

2.6 A Note on Robustness of the Design

The above example indicates that it is possible to systematically produce successful control system designs for uncertain plant using models with significant errors. The conservatism of the design depends upon the size of the modelling error but, in all cases, the procedure is robust in the sense that the controller will continue to stabilize the plant if, over a period of time, its dynamic characteristics change by less than a computable amount. More precisely, if G changes into the plant $\tilde{G}$ with step response $\tilde{Y}$, we can prove the following result:

Proposition 2: If the conditions of theorem 1 hold, then the closed-loop system of Fig. 1(a) will retain its stability if $\tilde{G}KF$ is controllable and observable, $\tilde{G} - G$ is stable and

$$N_\infty(\tilde{Y} - Y) < \frac{1 - \lambda_1\lambda_2}{\lambda_1} \qquad (37)$$

where λ_1 and λ_2 are as defined in lemma 1 and 2.

Proof: Simply verify that the conditions of lemma 1 hold with G replaced by $\tilde{G}$ and λ_2 replaced by $\tilde{\lambda}_2 = N_\infty(\tilde{Y} - Y_A)$. More precisely, noting that $N_\infty(\tilde{Y} - Y_A) \leqslant N_\infty(\tilde{Y} - Y) + N_\infty(Y - Y_A)$, (37) yields

$$\lambda_1 \tilde{\lambda}_2 \leq \lambda_1 (N_\infty (\tilde{Y} - Y) + \lambda_2) < 1 \tag{38}$$

---

3. Time Domain Design Based on Approximate Models

The procedures outlined in Section 2 have a striking similarity to well-known procedures but suffer from the general problem of frequency-domain technqiues i.e. it is difficult to make predictions concerning the details of the closed-loop transient performance. In particular, it is impossible to make confident predictions about the response characteristics of the real feedback scheme in terms of the response characteristics of the approximating feedback system except that it is stable and, if integrators are present, tracks step demands exactly and rejects step disturbances. Any design technique capable of resolving this problem (at least in part) must, intuitively, rely heavily on time-domain calculations. The general form of such a design aid is described in this section. The proof of the results relies on the use of functional analytic methods and hence, for simplicity of presentation, most of these are relagated to appendixes.

3.1 Time Domain Stability Theory and Performance Assessment

Suppose that the controller K has been designed to stabilize the plant approximation G_A and produce the desired response characteristics from the feedback system of Fig. 1(b). The method used is irrelevant to the following discussion but the use of the techniques of section 2 would, at least, produce a preliminary guarantee that K also stabilizes the real plant. The following result indicates how simple time domain/simulation methods can, under well-defined circumstances, be used as an alternative stability check and/or as a means of bounding the error in predicting transient performance.

<u>Theorem 2:</u> Suppose that the controller K has been designed (by some means) to stabilize the approximate model G_A in the feedback configuration of Fig. 1(b) and that the response $v_A(t)$ of the configuration of Fig. 8(a) from zero initial conditions to the demand input E(t) has been computed. Then the controller K will stabilize the real uncertain plant G in the configuration of Fig. 1(a) if

(a) the modelling error is stable (in the sense of (3)),

(b) the composite system GKF is controllable and observable

and if,

(c) either, defining $\lambda_4(t) \triangleq N_t(v_A)$, we have

$$\lambda_4(\infty) = N_\infty(v_A) < 1 \text{ or,} \tag{39a}$$

if $w_A(t)$ is the response from zero initial conditions of the feedback system of fig. 8(a) to a unit step demand input and $\lambda_4(t)$ is defined by $\lambda_4(t) \triangleq N_t(w_A)N_t(E)$, we have

$$\lambda_4(\infty) = N_\infty(w_A)N_\infty(E) < 1 \tag{39b}$$

Under these conditions, let $y_o(t)$ be the response of some proper, stable causal system H from zero initial conditions to a given piecewise continuous demand signal r(t). Then the responses y(t) and $y_A(t)$ of the real and approximating feedback schemes from zero initial conditions to the demand r(t) are related by the error bound

$$|y(t) - y_A(t)| \leqslant \varepsilon(t) \triangleq \frac{\lambda_4(t)}{1-\lambda_4(t)} \max_{o\leqslant t'\leqslant t} |y_A(t') - y_o(t')|$$
$$+ \frac{\lambda_5(t)}{1-\lambda_4(t)} \max_{o\leqslant t'\leqslant t} |r(t')| \quad , \quad t \geqslant o \tag{40}$$

where $\lambda_5(t) \triangleq N_t(z_A)N_t(E)$ and z_A is the response from zero initial conditions of the configuration of Fig. 8(b) to a unit step input. In particular, if r(t) is a unit step demand the bound can be improved to, in order of increasing conservatism

$$|y(t) - y_1(t)| \leq \varepsilon(t) \triangleq \frac{\lambda_4(t)}{1 - \lambda_4(t)} \max_{0 \leq t' \leq t} |y_1(t') - y_0(t')| \quad (41a)$$

$$|y(t) - y_A(t)| \leq \varepsilon(t) \triangleq \frac{\lambda_4(t)}{1 - \lambda_4(t)} \max_{0 \leq t' \leq t} |y_1(t') - y_0(t')| + |\eta(t)| \quad (41b)$$

$$|y(t) - y_A(t)| \leq \varepsilon(t) \triangleq \frac{\lambda_4(t)}{1 - \lambda_4(t)} \max_{0 \leq t' \leq t} |y_A(t') - y_0(t')| + \frac{1}{1 - \lambda_4(t)} \max_{0 \leq t' \leq t} |\eta(t')| \quad (41c)$$

where $y_1(t) = y_A(t) + \eta(t)$ and $\eta(t)$ is the response from zero initial conditions of the configuration of Fig. 8(b) to the input signal E(t).

Finally, both (40) and (41) hold with $\varepsilon(t)$ replaced by either

(i) $\varepsilon_\infty(t)$ derived by replacing $\lambda_4(t)$ and $\lambda_5(t)$ by $\lambda_4(\infty)$ and $\lambda_5(\infty)$ respectively or,

(ii) $\varepsilon_\mu(t)$ derived by replacing $\lambda_4(t)$ and $\lambda_5(t)$ by $\lambda_4(\mu_1(t))$ and $\lambda_5(\mu_2(t))$ respectively where each $\mu_k(t)$ is some function satisfying $\mu_k(t) \geq t$, for $t \geq 0$.

The theorem contains many possibilities in choice of H, choice of estimate and μ, as illustrated by the following remarks:

Choice of H: the stable system H is specified by the designer and, intuitively, can be used to decrease the uncertainty in the closed-loop response y(t) by reducing $\varepsilon(t)$. Three simple choices immediately suggest themselves

(i) the choice of $H = 0$ yields $y_o(t) = 0$, simplifies the configuration of Fig. 8(b), partially simplifies the form of the estimates (40) and (41), when $F = 1$, reduces simulation requirements as $v_A = \eta$ whereas

(ii) the choice of $H = F^{-1}$ (if F has a proper, stable inverse) yields the data $z_A(t) \equiv 0$, $\eta(t) \equiv 0$ and hence $\lambda_5(t) \equiv 0$ and $y_1(t) \equiv y_A(t)$ (the estimates (40) and (41) are identical in this case and two simulations are avoided), and

(iii) the choice of $H = (1 + G_A KF)^{-1} G_A K$ is equivalent to $y_o = y_A$ and (see appendix 9), as y_o is the first guess at y in a successive approximation scheme, it is envisaged that this choice will be the best of the three mentioned but at the expense of increased complexity of Fig. 8(b).

Choice of ε: The four estimates in (40) and (41) represent various degrees of pessimism. In general pessimism increases as we move from (41a) to (41b) to (41c) to (40) but simplicity increases at the same time. The choice of ε is therefore a compromise between accuracy and simplicity to suit the application and computing facilities available.

Choice of μ: Given a choice of estimate $\varepsilon(t)$, the choice of $\mu(t)=t$ yields the smallest error bounds but $\mu(t) = +\infty$ yields simplicity as the parameters $\lambda_4/(1-\lambda_4)$, $\lambda_5/(1-\lambda_4)$ and $1/(1-\lambda_4)$ are constant in (40) and (41). This simplicity is obtained at the expense of conservatism as $\varepsilon(t) \leq \varepsilon_\infty(t)$. A compromise can be reached by the use of other choices of μ. In particular the choice of $\mu(t) = t_k$ if $t_{k-1} \leq t < t_k$ (where $\{t_k\}$ are the stationary points of the signal considered) will need only estimates of the value and position of stationary points. This will be of particular importance if the signal has some noise content.

The proof of the theorem 2 is given in Appendix 9. It is useful however, to give the result the following step-by-step design interpretation.

Step 1: Obtain the plant response Y(t) from zero initial conditions to a unit step input.

Step 2: Choose an approximate plant model to fit plant characteristics to a convenient accuracy and to ensure that the modelling error $G - G_A$ is stable. Calculate $Y_A(t)$, $E(t)$ and hence $N_t(E)$.

Step 3: Design the controller K for $G_A(s)$ to obtain the required stability and performance characteristics from the approximating feedback system of Fig. 1(b). Any prefered technique can be used but the use of the technique of section 2 will have the advantage that the stability of the configuration Fig. 1(a) will be guaranteed at this early stage.

Step 4: Calculate the time response $v_A(t)$ or $w_A(t)$ and hence obtain $N_t(v_A)$ or $N_t(w_A)$. (Note that $w_A = z_A$ and $v_A = \eta$ if F=1 and H=0) If $\lambda_4(\infty) \geq 1$ the stability of the real feedback scheme Fig. 1(a) cannot be guaranteed unless the techniques of Section 2 are used in Step 3. If however $\lambda_4(\infty) < 1$ and GKF is both controllable and observable then we are guaranteed that the scheme will be asymptotically stable.

Step 5: If $\lambda_4(\infty) < 1$, choose a stable H and compute $\eta(t)$ or $z_A(t)$ to obtain an error bound $\varepsilon(t)$, $\varepsilon_\infty(t)$ or $\varepsilon_\mu(t)$ between the known performance of the approximating feedback system and the (as yet) unknown performance of the real feedback scheme for the demand signal of interest. Error bounds (40), (41b) and (41c) can be represented graphically by plotting the known response $y_A(t)$ and the 'boundary' responses $y_A(t) \pm \varepsilon(t)$ as shown in Fig. 9(a). The unknown response y(t) is known to lie in the band generated.

As $\varepsilon(t) \leqslant \varepsilon_{\mu}(t) \leqslant \varepsilon_{\infty}(t)$, the band $\varepsilon(t)$ will give the best estimate for finite, 'small' t but, as $t \to +\infty$, they are all identical as, from the definition $\varepsilon(t) - \varepsilon_{\infty}(t) \to o$ as $t \to +\infty$. The graphical interpretation of (41a) is illustrated in Fig. 9(b).

Step 6: If the design is regarded as unsatisfactory because, for example, the transient errors $\varepsilon(t)$ are larger than anticipated, the designer can either return to step 2 to choose a more accurate approximate model or attempt to reduce $\lambda_4(t)$ (and hence $\varepsilon(t)$) by reducing the control gains or changing H.

3.2 Illustrative Examples

3.2.1 Example 1: Consider the example of Section 2.5 with the proposed proportional controller $K(s) = K_1 = 1$. It was shown that the real plant is stable in the presence of this design and we can apply the above theory to assess performance degradation due to the approximation used. A simple calculation yields (with H = O)

$$w_A(t) = z_A(t) = \tfrac{1}{2}(1 + e^{-t}\cos t + e^{-t} \sin t) \tag{42}$$

and hence, after graphical analysis that $N(w_A) = N(z_A) = 1.57$ or (using equation (39b))

$$\lambda_4(\infty) = \lambda_5(\infty) = 1.57 \times 0.54 = 0.85 \tag{43}$$

Clearly $\lambda_4(\infty) < 1$ (confirming the stability predictions of Section 2.5) and the bound (40) can be written as $|y(t)-y_A(t)| \leqslant \varepsilon_{\infty}(t)$ where

$$\varepsilon_{\infty}(t) = 5.67 \max_{o \leqslant t' \leqslant t} |y_A(t')| + 5.67 \max_{o \leqslant t' \leqslant t} |r(t')| \tag{44}$$

Taking, for example, the case of a step input we clearly obtain the inequality, $\varepsilon_{\infty}(t) \geqslant 5.67$ for $t > o$ and hence that the bound (40) on prediction error allows the possibility of transient deviations of 500% of the magnitude of the demand signal. This bound is clearly of little practical value for predicting the detailed response characteristics in this particular example due to the magnitude of the modelling error employed.

A slightly better estimate of performance degradation using (40) can be obtained by the choice of $H = (1+G_A KF)^{-1} G_A K$ (when $y_o = y_A$) and the use of $\lambda_4(t) = N_t(v_A)$ rather than $\lambda_4(t) = N_t(w_A)N_t(E)$. In fact, after simulation investigation, it is easily verified that $\lambda_4(\infty) = 0.41$ and $\lambda_5(\infty) = 1.06$ from which

$$|y(t) - y_A(t)| \leqslant \varepsilon_\infty(t) = 1.8 \max_{o \leqslant t' \leqslant t} |r(t')| \tag{45}$$

predicting that we must anticipate prediction errors of up to 180% of the peak magnitude of the demand signal.

Finally, if r is a unit step, we obtain the tightest bounds from (41a) with $H = (1+G_A KF)^{-1} G_A K$ and the use of $\lambda_4(t) = N_t(v_A)$. In this case, equation (41a) has the form, for $t \geqslant o$,

$$|y(t) - (y_A(t) + \eta(t))| \leqslant \varepsilon(t) = \frac{\lambda_4(t)}{1-\lambda_4(t)} \max_{o \leqslant t' \leqslant t} |\eta(t')| \leqslant 0.12 \tag{46}$$

The form of η is shown in Fig. 10(a) and the error bounds illustrated graphically in Fig. 10(b), together with y and y_A.

3.2.2 Example 2: Suppose that a system has a known model defined by the transfer function

$$G(s) = \frac{20}{(s+1)(s+2)(s+10)} \tag{47}$$

and that a unity negative feedback proportional regulator design is to be attempted by using the approximate model

$$G_A(s) = \frac{2}{(s+1)(s+2)} \tag{48}$$

obtained by ignoring the fast mode. The step responses Y and Y_A together with E are shown in Fig. 11. Choosing the controller gain to produce a damping of $1/\sqrt{2}$ in the approximating feedback system of Fig. 1(b) yields the choice of $K(s) \equiv 1.25$ and excellent regulation properties.

The success of the design can be checked by simulation of the real feedback scheme. For illustrative purposes however, we will use the theorem 2 to guarantee stability and bound the performance degradation. Choosing, for simplicity $H = 0$ yields $y_o = o$ and $v_A(t) = \eta(t)$ as illustrated in Fig. 12(a). In particular we obtain after graphical analysis,

$$\lambda_4(\infty) = N_\infty(v_A) = 0.11 < 1 \tag{49}$$

and hence we conclude that the controller will stabilize the real plant if it is both controllable and observable. Performance deterioration can be assessed, for example, using (41a) to give, in the case of a unit step demand input,

$$|y(t) - (y_A(t)+\eta(t))| \leq \varepsilon(t) = \frac{\lambda_4(t)}{1-\lambda_4(t)} \max_{o<t'<t} |y_A(t)+\eta(t)|$$

$$\leq 0.07 \quad \forall \; t \geq o \tag{50}$$

The real and approximate responses to a unit step demand together with the error bounds are given in Fig. 12(b). There is clearly some pessimism here as the possibility of prediction errors of up to 13% of the steady state approximate response are predicted. This pessimism is not regarded as unduly large in this case bearing in mind the simplicity afforded by the choice of $H = 0$. Accuracy can be considerably improved by the choice of $H = (1 + G_A KF)^{-1} G_A K$ when $y_o = y_A$ and (41a) reduces to

$$\left|y(t) - y_1(t)\right| \leqslant \frac{\lambda_4(t)}{1-\lambda_4(t)} \max_{o \leqslant t' \leqslant t} \left|\eta(t')\right| \leqslant 0.0056 \quad (51)$$

which, in graphical terms, means that y is indistinguishable from y_1. This accuracy must be balanced agains the extra work and increased complexity involved in simulating the configuration of Fig. 8(b) to obtain η.

3.3 A Note on Robustness of the Design

The frequency-domain robustness analysis of section 2.5 carries through with virtually no change to the time-domain to yield the result:

Proposition 3: If all conditions of theorem 2 hold including (39b), then the closed-loop system of Fig. 1(a) will retain its stability with G replaced by $\tilde{G}$ if $\tilde{G}KF$ is controllable and observable, $G - \tilde{G}$ is stable and

$$N_\infty(Y-\tilde{Y}) < (1 - \lambda_4(\infty))/N_\infty(w_A) \quad (52)$$

3.4 On the Effect of Measurement Nonlinearities

The techniques described above can also be used to predict the stability and performance characteristics of the closed-loop system of Fig. 1(a) in the presence of a class of memoryless nonlinearities. More precisely, suppose that F is a scalar gain used in the approximating feedback scheme of Fig. 1(b) but that the real feedback scheme takes the form of Fig. 13 where the memoryless nonlinearity n takes the form

$$n(y) = F\,y + n_1(y) + n_2(y) \quad (53)$$

where $n_1(y)$ is a nonlinearity of finit incremental gain ν satisfying, for all y_1, y_2,

$$|n_1(y_1) - n_1(y_2)| \leqslant \nu|y_1 - y_2| \quad (54)$$

and $n_2(y)$ is a bounded-output nonlinearity of the form, for all y,

$$|n_2(y)| \leqslant q/2 \quad (55)$$

where $q \geqslant 0$ is a real scalar. Such nonlinearites have been discussed elsewhere(4,5) and represent a large class met in practice.

The basic result is stated below and is proved in Appendix 10.

Theorem 3: Suppose that the conditions of theorem 2 are satisfied and that the following responses have been computed,

(a) the response Y_A^C from zero initial conditions of the linear system of Fig. 1(b) to a unit step input, and

(b) the response y_A^H from zero initial conditions of the linear system of Fig. 14 to a unit step input (Note: $Y_A^C = y_A^H$ if $H = 0$)

Then the controller K will stabilize the unknown system G in the configuration of Fig. 13 if, defining $\lambda_6(t) \triangleq \lambda_7(t)\,\nu$ with

$$\lambda_7(t) = N_t(Y_A^C) + \frac{\lambda_4(t)}{1-\lambda_4(t)} \quad N_t(y_A^H) + \frac{\lambda_5(t)}{1-\lambda_4(t)}\;, \tag{56}$$

we have

$$\lambda_6(\infty) < 1 \tag{57}$$

Under these conditions and assuming that $n_1(0) = 0$, the responses $y_{n\ell}(t)$ and $y_A(t)$ of the real, nonlinear and approximating linear feedback system from zero initial conditions to the same bounded and piecewise continuous demand input $r(t)$ are related by

$$|y_{n\ell}(t) - y_A(t)| \leqslant \varepsilon_{n\ell}(t)$$

$$\triangleq \frac{\lambda_6(t)\lambda_7(t)}{1-\lambda_6(t)} \quad \max_{0\leqslant t'\leqslant t} |r(t')| + \varepsilon(t) + \frac{\lambda_7(t)}{1-\lambda_6(t)} \; \frac{q}{2} \tag{58}$$

where $\varepsilon(t)$ is as given in equation (40). Moreover, if r is a unit step input, (58) holds with ε as given in (41b) or (41c) and (41a) is replaced by

$$|y_{n\ell}(t)-y_1(t)| \leqslant \varepsilon_{n\ell}(t) \triangleq \frac{\lambda_6(t)\lambda_7(t)}{1-\lambda_6(t)} \quad \max_{0\leqslant t'\leqslant t} |r(t')| + \varepsilon(t) + \frac{\lambda_7(t)}{1-\lambda_6(t)} \; \frac{q}{2} \tag{59}$$

with ε as defined in (41a).

Finally both (58) and (59) are valid with $\varepsilon_{n\ell}(t)$ replaced by either $\varepsilon^{\infty}_{n\ell}(t)$ (obtained from $\varepsilon_{n\ell}(t)$ by replacing $\lambda_4(t), \lambda_5(t), \lambda_6(t)$ and $\lambda_7(t)$ by these values at $t = \infty$) or $\varepsilon^{\mu}_{n\ell}(t)$ (obtained by replacing $\lambda_k(t)$, $4 \leq k \leq 7$, by $\lambda_k(\mu_k(t))$, $4 \leq k \leq 7$, where each μ_k satisfies $\mu_k(t) \geq t$, $t \geq o$).

The interpretation of the error bounds in graphical terms is identical to that outlined after theorem 2 and the choice of H, ε and μ appears to be governed by the same rules. Note however that, for any given choice of $\varepsilon(t)$ for the linear part of the analysis, we have $\varepsilon^{\infty}_{n\ell}(t) \geq \varepsilon^{\mu}_{n\ell}(t) \geq \varepsilon_{n\ell}(t) \geq \varepsilon(t)$ indicating that the introduction of the nonlinearity increases the uncertainty surrounding the response of the closed-loop system. Finally note that $\lambda_6(\infty)$ reaches its minimum value with respect to H when $y^H_A = O$ i.e. when $H = (1 + G_A KF)^{-1} G_A K$.

4. Controller Design for Discrete Plant using Approximate Models

All of the theory and design concepts described above are easily extended to cover the case of a discrete plant G with synchronous output sampling and control actuation and the use of a discrete approximate model. For this reason, only the general outlines are given here.

The problem considered is the design of a proper, rational controller K in Fig. 1(a) for the uncertain plant G in the presence of proper, rational measurement dynamics F. All elements are linear and discrete with synchronous input/output behaviour. We suppose that the output sequence $Y = \{Y_o, Y_1, Y_2 \ldots\ldots\}$ generated by the plant from zero initial conditions to a unit step input is known and that a linear, discrete approximate model has been constructed. We denote by $Y_A = \{Y_{AO}, Y_{A1}, \ldots\}$ the step response of this model. The error sequence $E = \{E_o, E_1, \ldots\}$ is defined by $E_k = Y_k - Y_{Ak}$, $k \geqslant o$.

It is assumed that both G and G_A can be represented by convolution operators, $k \geqslant o$

$$y_k = \sum_{j=1}^{k} H_j\, u_{k-j} \quad , \quad (y_A)_k = \sum_{j=1}^{k} H_j^A u_{k-j} \tag{60}$$

with stable modelling error in the sense that

$$\sum_{k=1}^{\infty} |H_k - H_k^A| < +\infty \tag{61}$$

Clearly, for $k \geqslant o$,

$$Y_k = \sum_{j=1}^{k} H_j \ , \ Y_{Ak} = \sum_{j=1}^{k} H_j^A \tag{62}$$

and the signal $E = Y - Y_A$ is stable.

If the controller K successfully stabilizes G_A we have

$$\inf_{1 \leqslant |z| \leqslant R} |1 + G_A(z)K(z)F(z)| > 0 \tag{63}$$

(where R is some suitably large number) and K will also successfully stabilize G if

$$\inf_{1 \leqslant |z| \leqslant R} \left| 1 + G(z)K(z)F(z) \right| > 0 \tag{64}$$

Comparing these equations with (6) and (7) indicates that lemma 1 holds in the discrete case if the D contour is replaced by the two circles $|z| = 1$ and $|z| = R$ and the region Res $\geqslant$ o by the region $1 \leqslant |z| \leqslant R$.

Frequency response bounds can be obtained from transient data in a similar manner to that described in Section 2.2. More precisely, the following result can be proved in a similar manner to Proposition 1:

Proposition 4: If the sequence $f_o = d$ and

$$f_k \triangleq d + \sum_{j=1}^{k} g_j \quad , \quad k \geqslant 1 \tag{65}$$

is bounded with local maxima or minima at sample instants $1 \leqslant k_1 < k_2 \quad .....$ in the extended positive integers, then, taking $k_o = o$, we have

$$|d| + \sum_{j=1}^{k} |g_j| = N_k(f) \tag{66}$$

where

$$N_k(f) = |f_o| + \sum_{j=1}^{k^*(k)} |f_{k_j} - f_{k_{j-1}}| + |f_k - f_{k^*(k)}| \;\ldots \tag{67}$$

where $k^*(k)$ is the largest integer $k_1, k_2, \ldots,$ satisfying $k_j < k$.

This result has a similar graphical interpretation to that of Proposition 1. Our main concern here however is that both lemma 2 and theorem 1 hold with the region Res $\geqslant$ o replaced by $1 \leqslant |z| \leqslant R$ and the imaginary axis $s = i\omega$, $\omega \geqslant o$, replaced by the unit circle $z = e^{i\theta}$, $-\pi < \theta < o$. These results could form the basis of a frequency domain design procedure similar to that outlined in section 2.4 and Proposition 2 is still valid indicating that the design is robust in a well-defined sense.

Finally we note that all of the time domain results of section 3 carry over to the discrete case by replacing $L_\infty(o,+\infty)$ by the Banach space ℓ_∞ of uniformly bounded real sequences $\{y_o, y_1, \ldots\}$ with norm $||y|| = \sup_{k \geq o} |y_k|$ and by replacing continuous signals by their sampled counterpart (e.g. $u_A(t)$ in theorem 2 is replaced by $u_A = \{u_{AO}, u_{A1}, \ldots\}$). The stability conditions (39) and (56) remain unchanged but the transient error bounds must be expressed in discrete form. For example, (40) will read

$$|y_k - (y_A)_k| \leq \varepsilon_k \quad , \quad k \geq o \tag{68}$$

with

$$\varepsilon_k = \frac{\lambda_4(k)}{1-\lambda_4(k)} \max_{o \leq k' \leq k} |(y_A)_{k'} - (y_o)_{k'}| + \frac{\lambda_5(k)}{1-\lambda_4(k)} \max_{o \leq k' \leq k} |r_{k'}| \tag{69}$$

The detailed proof of these results is straightforward and hence omitted.

5. Conclusions

Frequency response methods for the analysis and design of feedback control systems for both scalar and multivariable plant are now well-established(6-10) and can give excellent feedback designs that are robust to modelling errors if, for example, standard gain and phase margin guidelines are observed. These ideas are successful if plant uncertainty is not too great, but, if the plant model is rather crude, they cannot be used with confidence. Several techniques have been suggested to cope with this problem ranging, for example, from the detailed work of Horowitz[11] to the more qualitative work of Davison[12], Porter[13] and Koivo[14] and the important special cases considered by Owens et al[2,4,15-17] and Astrom[18]. All these contributions differ in scope and emphasis but none provide an explicit relationship between the observed errors between plant and model open-loop performance and the required stability of the implemented feedback scheme. This problem has been the topic of this paper.

The crucial starting point of the analysis is the assumption that a plant step response can be synthesized from plant tests or simulations of a complex model. Given this data the computed error between plant and approximate model step responses can be used to compute a single numerical measure $N_t(E)$ of the errors involved. If design is to proceed on the basis of frequency response analysis, this measure can be used to construct a 'confidence band' around the approximate model inverse Nyquist plot and encirclements of this band around the (-1,0) point can be used to guarantee stability of the implemented feedback scheme. The confidence band is generated by the union of 'confidence circles' at each frequency point that are reminiscent of the Gershgorin circles of the inverse Nyquist array[6-8] and dyadic expansion[7,8] design methods for multivariable systems. The width of the confidence band is, roughly speaking, a measure of the modelling error and, by suitable choice of approximate model, this can be chosen to provide the required compromise between accuracy of theoretical predictions and the simplicity afforded by a simple, but possibly crude, approximate model. This feature is regarded as an important bonus in design work.

Another important bonus following from the type of analysis used is that, under certain well-defined conditions, the degradation in transient performance due to known modelling erros can be bounded in terms of $N_t(E)$ and computable characteristics of the approximating feedback scheme even if measurement nonlinearities are present. These results can be regarded as an extension of the frequency-domain design results or they can be regarded as a basis for design based on trial-and-error simulation procedures alone.

Finally, in general terms, it would appear that stability in the presence of severe plant and model discrepancies can be guaranteed as illustrated by the examples in section 2.5.. Also, in well-defined circumstances (Theorem 2), estimates of performance degradation can be found but, as seen in section 3.2.1., these error bounds can be so large as to be of little practical value. In general terms, if tight transient error bounds are desired then both λ_4 and λ_5 should be small when compared with unity, i.e. we must either choose our approximate model G_A to made $N_\infty(E)$ small and/or we must reduce the magnitude of $N_t(w_A)$ or $N_t(v_A)$ by using low-gain controllers. If neither of these solutions are acceptable then some other theoretical bound should be derived. This problem is presently under consideration.

6. Acknowledgements

This work is supported by SERC under grant GR/B/23250.

7. References

(1) D.H. Owens, A. Chotai: 'Robust controller design for uncertain dynamic systems using approximate models: Part II Multivariable Systems'

(2) D.H. Owens, A. Chotai: 'Controller design for unknown multivariable systems using monotone modelling errors' Proc. IEE, Pt. D., to appear.

(3) W. Rudin: 'Principles of mathematical analysis' (2nd Edition) McGraw-Hill, 1964.

(4) D.H. Owens: 'On the effect of nonlinearities in multivariable process control', Proceedings of IEE Int. Conf. 'Control and its Applications', Univ. Warwick, March 1981, 240-244.

(5) D.H. Owens, A. Chotai: 'Robust stability of multivariable feedback systems subject to linear and nonlinear feedback perturbations'. To appear IEEE Trans. Aut. Contr., February 1982.

(6) H.H. Rosenbrock: 'Computer-aided design of control systems', Academic Press, 1974.

(7) D.H. Owens: 'Feedback and multivariable systems', Peter Peregrinus, 1978.

(8) A.G.J. MacFarlane: 'Frequency response methods in control systems', IEEE Press, 1979.

(9) A.G.J. MacFarlane: 'Complex variable methods for linear multivariable feedback systems', Taylor and Francis, 1980.

(10) D.H. Owens: 'Multivariable and optimal systems', Academic Press, 1981.

(11) I.M. Horowitz, M. Sidi: 'Synthesis of feedback systems with large plant ignorance for prescribed time-domain tolerances', Int. J. Contr., 16, 1972, 287-309.

(12) E.J. Davison: 'Multivariable tuning regulators: the feedforward and robust control of a general servomechanism problem', IEEE Trans. Aut. Contr., AC-21, 1976, 35-47.

(13) B. Porter: 'Design of error-actuated controllers for unknown multivariable plants', Electronics Letters, 17(3), 1981, 106-107.

(14) J. Pentinnen, H.N. Koivo: 'Multivariable tuning regulators for unknown systems', Automatica, 1980, 16, 393-398.

(15) J.B. Edwards, D.H. Owens: 'First-order models for multivariable process control', Proc. IEE, 1977, 124, 1083-1088.

(16) D.H. Owens: 'Discrete first-order models for multivariable process control', Proc. IEE, 1979, 126, 525-530.

(17) D.H. Owens, A. Chotai: 'Simple models for robust control of unknown or badly-defined systems'. In 'self-tuning and Adaptive Control', (Ed. S.A. Billings and C.J. Harris), Peter Peregrinus, 1981.

(18) K.J. Åstrom: 'A robust sampled regulator for stable systems with monotone step responses', Automatica, 1980, 16, 313-315.

(19) M. Vidyasagar: 'Nonlinear systems analysis', Prentice-Hall, 1978.

(20) M. Vidyasagar: 'Input-output analysis of large-scale interconnected systems', Springer-Verlag, 1981.

Appendices

8. Numerical Evaluation of N(E)

Although the procedure implicit in Proposition 1 is well-defined, it is important to know the effect of finite data records and errors in estimation of the stationary points $t_1, t_2, \ldots$. The following result simply states that, if data records are long enough, $N_\infty(f)$ can be estimated to an arbitrary accuracy.

Proposition 5: Suppose that $N_\infty(f)$ is finite. Then given any $\varepsilon > o$ there exists a time $T' \geqslant 0$ such that knowledge of $f(t)$ on any interval $[0,T]$ with $T \geqslant T'$ ensures that the numerical estimate of $N_\infty(f)$ defined by

$$N_T(f) = |f(T) - f(t_{k^*})| + \sum_{1 \leqslant k \leqslant k^*} |f(t_k) - f(t_{k-1})| + |f(o+)| \tag{70}$$

(where k^* is the largest index such that $t_k < T$) satisfies the accuracy relation

$$N_\infty(f) - \varepsilon \leqslant N_T(f) \leqslant N_\infty(f) \tag{71}$$

Proof: As $N_\infty(f)$ is finite by assumption, then there exists T' such that

$$\int_T^\infty |g(t)|dt \leqslant \varepsilon \tag{72}$$

for all $T \geqslant T'$ and hence that

$$N_\infty(f) - \varepsilon \leqslant |d| + \int_o^T |g(t)|dt \leqslant N_\infty(f) \tag{73}$$

for all $T \geqslant T'$. The result is now proved as, by Proposition 1,

$$N_T(f) = |d| + \int_o^T |g(t)|dt \tag{74}$$

The problem of errors in estimation of the stationary points t_k, $k \geq 1$, is best resolved by a combination with the finite-data record problem i.e.

Proposition 6: Suppose $\varepsilon > o$ is an arbitrary accuracy parameter and that $f(t)$ is known on the interval $o \leq t \leq T$ where $N_\infty(f) - \varepsilon/2 \leq N_T(f) \leq N_\infty(f)$. Then there exists a maximum permitted error $\delta > o$ such that, if the estimates t'_k of the t_k satisfying $t_k \leq T$ satisfy $|t_k - t'| \leq \delta$ then the estimate

$$N'(f,T) \triangleq |f(T) - f(t'_{k^*})| + \sum_{1 \leq k \leq k^*} |f(t'_k) - f(t'_{k-1})| + |f(o+)| \tag{75}$$

satisfies the accuracy relation

$$N_\infty(f) - \varepsilon \leq N'(f,T) \leq N_\infty(f) \tag{76}$$

Proof: By the continuity of f, there exists $\delta > o$ such that $|N_T(f) - N'(f,T)| < \varepsilon/2$ if the t_k are estimated to accuracy better than δ. The result now follows trivially as a simple graphical argument yields the observation that $N'(f,T) \leq N_T(f)$ and hence that

$$N_\infty(f) \geq N'(f,T) = N_T(f) + N'(f,T) - N_T(f)$$

$$\geq N_\infty(f) - \varepsilon/2 - \varepsilon/2 = N_\infty(f) - \varepsilon \tag{77}$$

as required.

One immediate and interesting corollary can be roughly stated as follows:

Corollary: Let $f_k \triangleq f(kh)$, $k \geq o$, be the data sequence obtained by sampling $f(t)$ at the sampling rate h^{-1} on $o \leq t \leq T$ as defined above. Then, for each $\varepsilon > o$, there exists $h^* > o$ such that, for all sampling rates $h^{-1} \geqslant (h^*)^{-1}$, the estimate of $N_\infty(f)$ is in error by at most ε.

Proof: The sampled data sequence $\{f_o, f_1, \ldots\}$ can be used to estimate the t_k to an accuracy of, at worst, the sample interval h. Let $h^*\delta = 1$ with δ as in Proposition 6.

In effect, the result states that $N_\infty(f)$ can always be accurately estimated using long enough data sequence and fast data sampling. Unfortunately, there are no known means of assessing what is 'long enough' or 'fast enough' in a given application. This is a problem of judgement for the given data and problem .

9. Proof of Theorem 2

To prove this result, we regard the stability problem as an input-output[19,20] stability problem in $L_\infty(o,\infty)$. We denote by $L_\infty^{ext}(o,\infty)$ the extended space[19] of $L_\infty(o,\infty)$ and by $P_T f$, the natural projection of $f \in L_\infty^{ext}$ into $L_\infty(O,T)$ (regarded as a subspace of $L_\infty(o,\infty)$). Note that $P_\infty f = f$. It is well-known[20] that any bounded mapping L of $L_\infty(O,\infty)$ into itself of the form $y = L\,u$ with the convolution description,

$$y(t) = d\,u(t) + \int_o^t g(t')\,u(t-t')dt' \qquad (78)$$

is causal and, for any $T \geqslant O$ (including $T = +\infty$) , $P_T L$ has norm

$$\| P_T L \|_\infty = |d| + \int_o^T |g(t)|dt \qquad (79)$$

Comparing with Proposition 1, we conclude that

$$\| P_T L \|_\infty = N_T(f) \quad , \quad T > O \qquad (80)$$

provided that the 'step response' f of L (i.e. the image of the unit function) is nicely behaved (i.e. continuous with only a finite number of maxima and minima on any finite interval). This technique for evaluating norms using step response data will be used several times in the following proof.

Assuming zero initial conditions, and regarding G, G_A, K and F as causal, linear mappings of L_∞^{ext} into itself, the feedback system of Fig. 1(a) can be written as the equation

$$y = GK\,r - GKF\,y \tag{81}$$

in L_∞^{ext}. Adding $G_A\,K\,F\,y$ to both sides of the equation and noting that the stability of Fig. 1(b) ensures that $1 + G_A\,K\,F$ is invertible, we obtain, after a little manipulation and using the commutation properties of scalar convolution operators,

$$y = (1 + G_A KF)^{-1} GKr - (1 + G_A KF)^{-1} KF(G-G_A)y \tag{82}$$

The configuration is input/output stable if this equation has a solution $y \in L_\infty(0,\infty)$ for every demand input $r \in L_\infty(o,\infty)$. Applying the global contraction mapping theorem[19], this will certainly be the case if the two operators $(1 + G_A KF)^{-1} G_A K$ and $(1+G_A KF)^{-1} KF\ (G-G_A)$ are bounded maps of $L_\infty(o,\infty)$ into itself and

$$||(1 + G_A KF)^{-1} KF(G-G_A)||_\infty < 1 \tag{83}$$

The stability of Fig. 1(b) ensures the boundedness of $(1 + G_A KF)^{-1} G_A K$, $(1 + G_A KF)^{-1} K$ and $(1 + G_A KF)^{-1} KF$ and $G - G_A$ is stable and hence bounded by assumption. Applying (80) to $L = (1 + G_A KF)^{-1} KF(G-G_A)$ with $T = +\infty$ yields

$$||(1 + G_A KF)^{-1} KF(G-G_A)||_\infty = N_\infty(v_A) \tag{84}$$

where v_A is the response of L from zero initial conditions to a unit step input $\xi(t)$. But $v_A = L\xi = (1+G_A KF)^{-1} KF(G-G_A)\xi = (1+G_A KF)^{-1} K\,F\,E$ as $E = (G-G_A)\xi$ by definition. Remembering the commutativity properties of scalar convolution operators, it follows that v_A is the response from zero initial conditions of the configuration of Fig. 8(a) to the drive input E(t). The stability condition (83) now reduces to (39a) as required. It can be relaxed to (39b) by noting that (83) is implied by

$$||(1 + G_A KF)^{-1} KF||_\infty . ||G-G_A||_\infty < 1 \tag{85}$$

and that $||(1 + G_A KF)^{-1} KF||_\infty = N_\infty(w_A)$ with $||G-G_A||_\infty = N_\infty(E)$. Our stability proof concludes with the observation that suitable controllability and observability assumptions convert input-output stability results into results on asymptotic stability.

Given the contraction condition (83) or (85), the solution of (82) can be obtained by successive approximation. Take as the initial guess $y_o = Hr \in L_\infty(o,\infty)$ and applying the projection P_t to (82) yields the first iterate

$$P_t\, y_1 = P_t(1 + G_A KF)^{-1} G_A K\, r + P_t(1+G_A KF)^{-1} K(1-FH) P_t (G-G_A) P_t r$$

$$= P_t\, y_A + P_t \eta \qquad (86)$$

where

$$\eta = (1 + G_A KF)^{-1} K\,(1-FH)(G-G_A) r \qquad (87)$$

If r is a unit step then $(G-G_A)r = E$ and η is hence the response from zero initial conditions of the configuration of Fig. 8(b) to the input E(t). Standard successive approximation formulae then yield the estimate

$$||P_t(y-y_1)||_\infty \leq \frac{\lambda_4(t)}{1 - \lambda_4(t)} ||P_t(y_1-y_o)||_\infty \qquad (88)$$

where $\lambda_4(t)$ is simply $||P_t(1+G_A KF)^{-1} KF(G-G_A)||_\infty = N_t(v_A)$ (if (39a) holds) or the more conservative $||P_t(1+G_A KF)^{-1} KF||_\infty . ||P_t(G-G_A)||_\infty = N_t(w_A) N_t(E)$ (if 39b holds). This proves (41a) whilst (41b) and (41c) follow from the triangle inequality. If r is not a unit step (88) still holds but η cannot be computed without detailed knowledge of G. A more conservative result is obtained using the bound

$$||P_t \eta||_\infty \leq ||P_t(1+G_A KF)^{-1} K(1-FH)||_\infty . ||P_t(G-G_A)||_\infty . ||P_t r||_\infty$$

$$= N_t(z_A) N_t(E) ||P_t r||_\infty = \lambda_5(t) ||P_t r||_\infty \qquad (89)$$

following from the definition of z_A and the identification (80). Using (88) with $y_1 = y_A + \eta$ then gives

$$||P_t(y - y_A)||_\infty \leqslant ||P_t(y - y_1)||_\infty + ||P_t(y_1 - y_A)||_\infty$$

$$\leqslant \frac{\lambda_4(t)}{1 - \lambda_4(t)} ||P_t(y_A + \eta - y_o)||_\infty + ||P_t\eta||_\infty$$

$$\leqslant \frac{\lambda_4(t)}{1 - \lambda_4(t)} ||P_t(y_A - y_o)||_\infty + \{\frac{\lambda_4'(t)}{1 - \lambda_4(t)} + 1\} ||P_t\eta||_\infty \qquad (90)$$

Equation (40) follows from the definition of $||\cdot||_\infty$ after a little manipulation, the use of (89) and the observation that $|y(t) - y_A(t)| \leqslant ||P_t(y-y_A)||_\infty$.

Finally, the replacement of $\lambda_4(t)$ and $\lambda_5(t)$ by $\lambda_4(\mu_1(t))$ and $\lambda_5(\mu_2(t))$ respectively or $\lambda_4(\infty)$ and $\lambda_5(\infty)$ respectively is possible as $\lambda_4(t)$ and $\lambda_5(t)$ are monotonically increasing in $[o,\infty)$ and $1/(1-\lambda)$ is monotonically increasing in the interval $o \leqslant \lambda < 1$.

10. Proof of Theorem 3

Theorem 3 is proved in a similar manner to theorem 2 by writing the closed-loop equations of the system as

$$y_{n\ell} = GK(r - (Fy_{n\ell} + n_1(y_{n\ell}) + n_2(y_{n\ell}))) \qquad (91)$$

or, if L_c is the linear operator in $L_\infty(o,\infty)$ defined by Fig.1(a),

$$y_{n\ell} = L_c(r - n_1(y_{n\ell}) - n_2(y_{n\ell})) \qquad (92)$$

The proof can now proceed in a similar manner to that found in ref. (5) and is outlined below. Regarding $r - n_2(y_{n\ell}) \in L_\infty$ as fixed, the contraction mapping theorem proves that a unique solution $y_{n\ell} \in L_\infty$ exists for every $r \in L_\infty$ if we can choose a real number μ satisfying

$$||L_c||_\infty \nu \leqslant \mu < 1 \qquad (93)$$

Using the boundedness relation $||P_t y_A||_\infty \leq ||P_t L_C^A||_\infty \cdot ||P_t r||_\infty$ where L_C^A is the operator in $L_\infty(o,\infty)$ represented by Fig. 1(b), we see that $||P_t L_C^A||_\infty = N_t(Y_A^C)$ and $|y_A(t)| \leq ||P_t y_A||_\infty \leq N_t(Y_A^C)||P_t r||_\infty$ (94)

Using $y_o = Hr$, (40) implies that

$$|y(t)| \leq |y_A(t)| + |y(t) - y_A(t)|$$

$$\leq N_t(Y_A^C)||P_t r||_\infty + \frac{\lambda_4(t)}{1 - \lambda_4(t)}||P_t(y_A - y_o)||_\infty$$

$$+ \frac{\lambda_5(t)}{1 - \lambda_4(t)} \; ||P_t r||_\infty \tag{95}$$

or, as

$$||P_t(y_A - y_o)||_\infty = ||P_t((1+G_A KF)^{-1} G_A K - H)r||_\infty$$

$$\leq ||P_t((1+G_A KF)^{-1} G_A K - H)||_\infty \cdot ||P_t r||_\infty$$

$$= N_t(y_A^H)||P_t r||_\infty \tag{96}$$

(from the definition of y_A^H and (80)), we obtain

$$||P_t L_c||_\infty \leq \lambda_7(t) \tag{97}$$

Clearly, (57) implies (93) with $\mu = \lambda_7(\infty)\nu$. Stability is hence proved.

Applying standard successive approximation procedures with zero initial guess yields the first iterate $y_{n\ell}^{(1)} = L_c(r - n_2(y_{n\ell})) = y - L_c n_2(y_{n\ell})$

$$||P_t(y_{n\ell} - y_{n\ell}^{(1)})||_\infty \leq \frac{\lambda_6(t)}{1 - \lambda_6(t)} \; ||P_t y_{n\ell}^{(1)}||_\infty \tag{98}$$

leading to

$$||P_t(y_{n\ell}-y)||_\infty \leq ||P_t(y_{n\ell}-y_{n\ell}^{(1)})||_\infty + ||P_t(y_{n\ell}^{(1)}-y)||_\infty$$

$$\leq \frac{\lambda_6(t)}{1-\lambda_6(t)} ||P_t\, y_{n\ell}^{(1)}||_\infty \qquad + ||P_t(y_{n\ell}^{(1)} - y)||_\infty$$

$$\leq \frac{\lambda_6(t)}{1-\lambda_6(t)} \quad ||P_t y||_\infty + \left(\frac{\lambda_6(t)}{1-\lambda_6(t)} + 1\right) ||P_t(y_{n\ell}^{(1)} - y)||_\infty$$

$$\leq \frac{\lambda_6(t)\lambda_7(t)}{1-\lambda_6(t)} \quad ||P_t r||_\infty + \frac{\lambda_7(t)}{1-\lambda_6(t)} \quad \frac{q}{2} \tag{99}$$

as $||P_t y||_\infty \leq \lambda_7(t)\ ||P_t r||_\infty$ and $||P_t(y_{n\ell}^{(1)} - y)||_\infty = ||P_t L_c n_2(y_{n\ell})||_\infty$ $\leq ||P_t L_c||_\infty \cdot ||n_2(y_{n\ell})||_\infty \leq \lambda_7(t)q/2$. It follows that

$$||P_t(y_{n\ell}- y_A)||_\infty \leq ||P_t(y_{n\ell} - y)||_\infty + ||P_t(y - y_A)||_\infty$$

$$\leq \frac{\lambda_6(t)\lambda_7(t)}{1 - \lambda_6(t)} \quad ||P_t r||_\infty + \frac{\lambda_7(t)}{1 - \lambda_6(t)} \quad \frac{q}{2} + \varepsilon(t) \tag{100}$$

which implies (58) trivially. Equation (59) follows in a similar manner.

Finally, the validity of the bounds $\varepsilon_{n\ell}^{\infty}(t)$ and $\varepsilon_{n\ell}^{\mu}(t)$ follows in a similar manner to the proof in theorem 2 from the monotonicity properties of $\lambda_4, \lambda_5, \lambda_6, \lambda_7$ and $1/(1-\lambda)$.

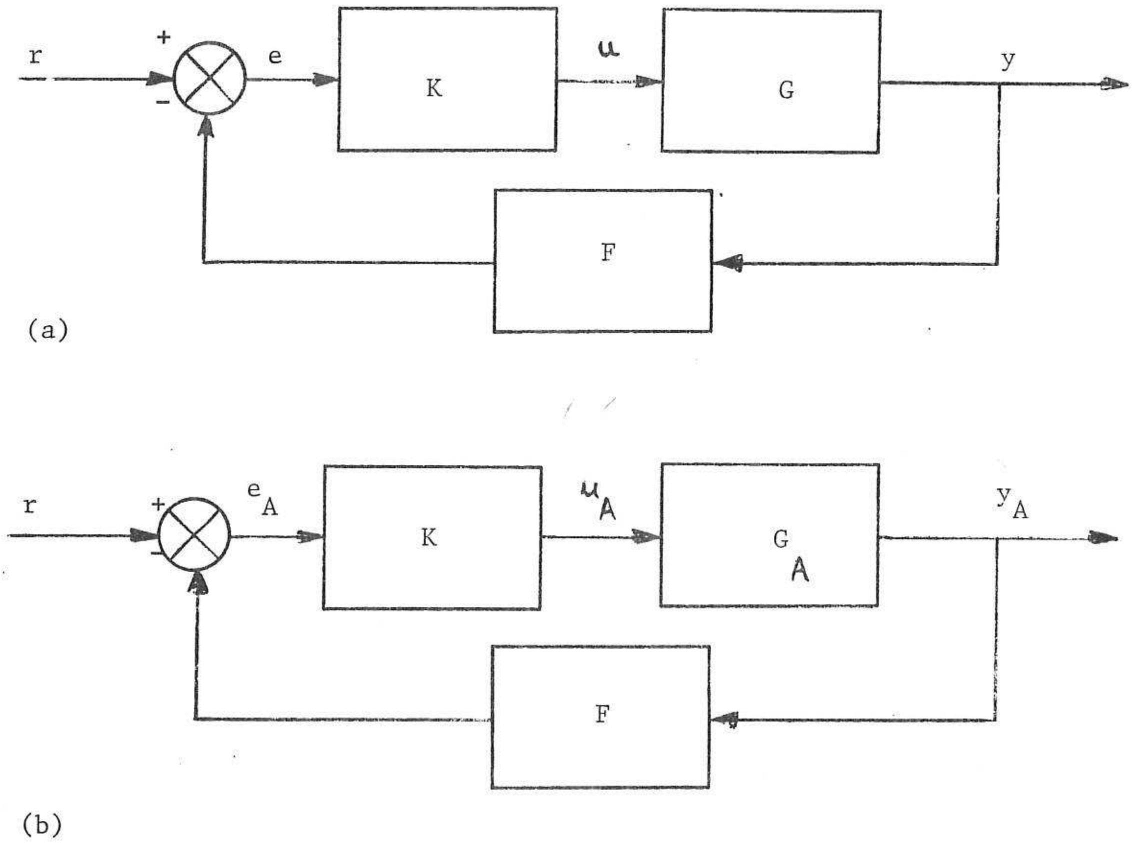

Fig. 1 (a) Real and (b) Approxmating Feedback Systems

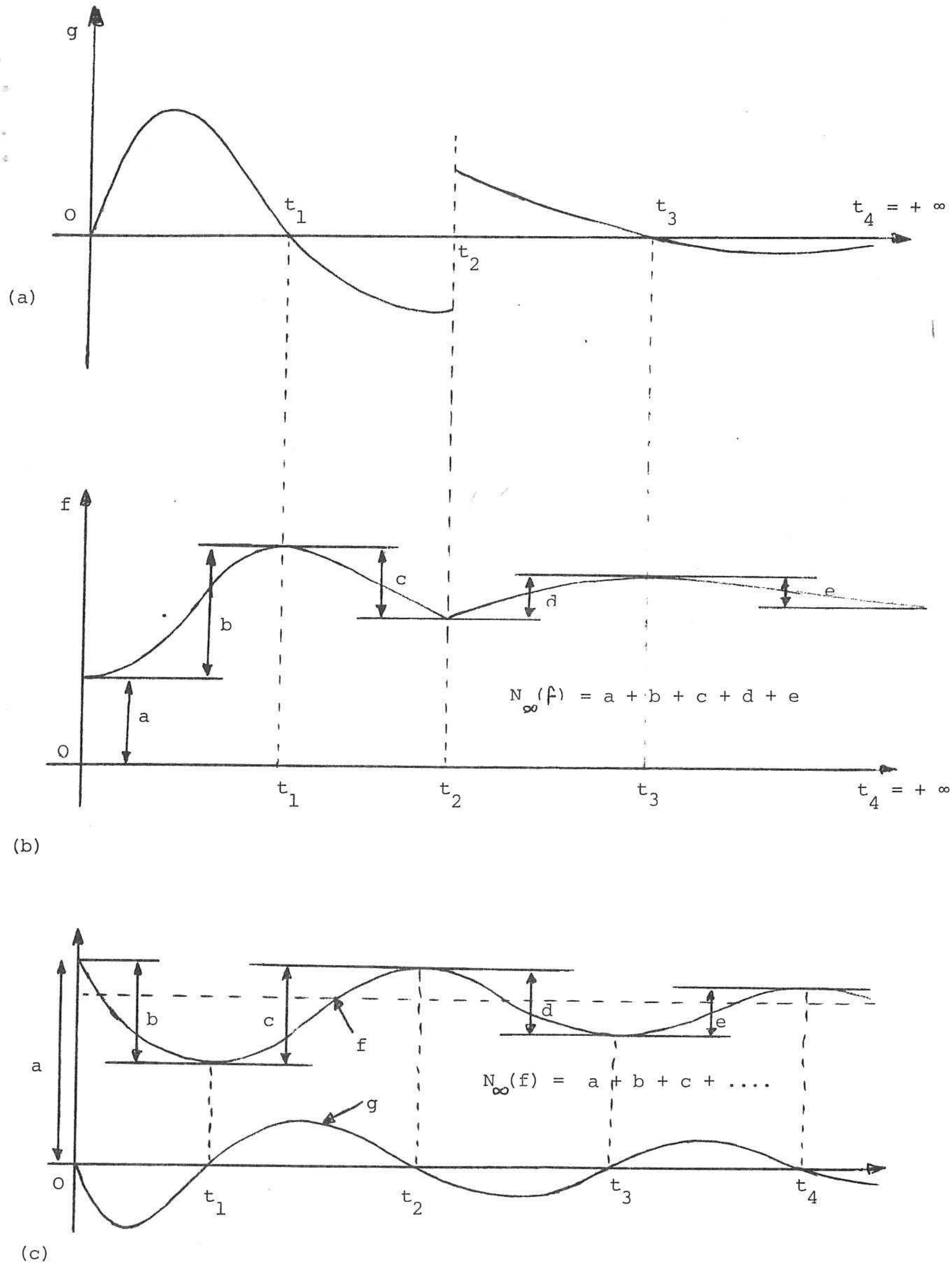
g
O
t_1
t_2
t_3
$t_4 = +\infty$
(a)
f
b
c
d
e
a
$N_\infty(f) = a + b + c + d + e$
O
t_1
t_2
t_3
$t_4 = +\infty$
(b)
a
b
c
d
e
f
g
$N_\infty(f) = a + b + c + \ldots.$
O
t_1
t_2
t_3
t_4
(c)

Fig. 2

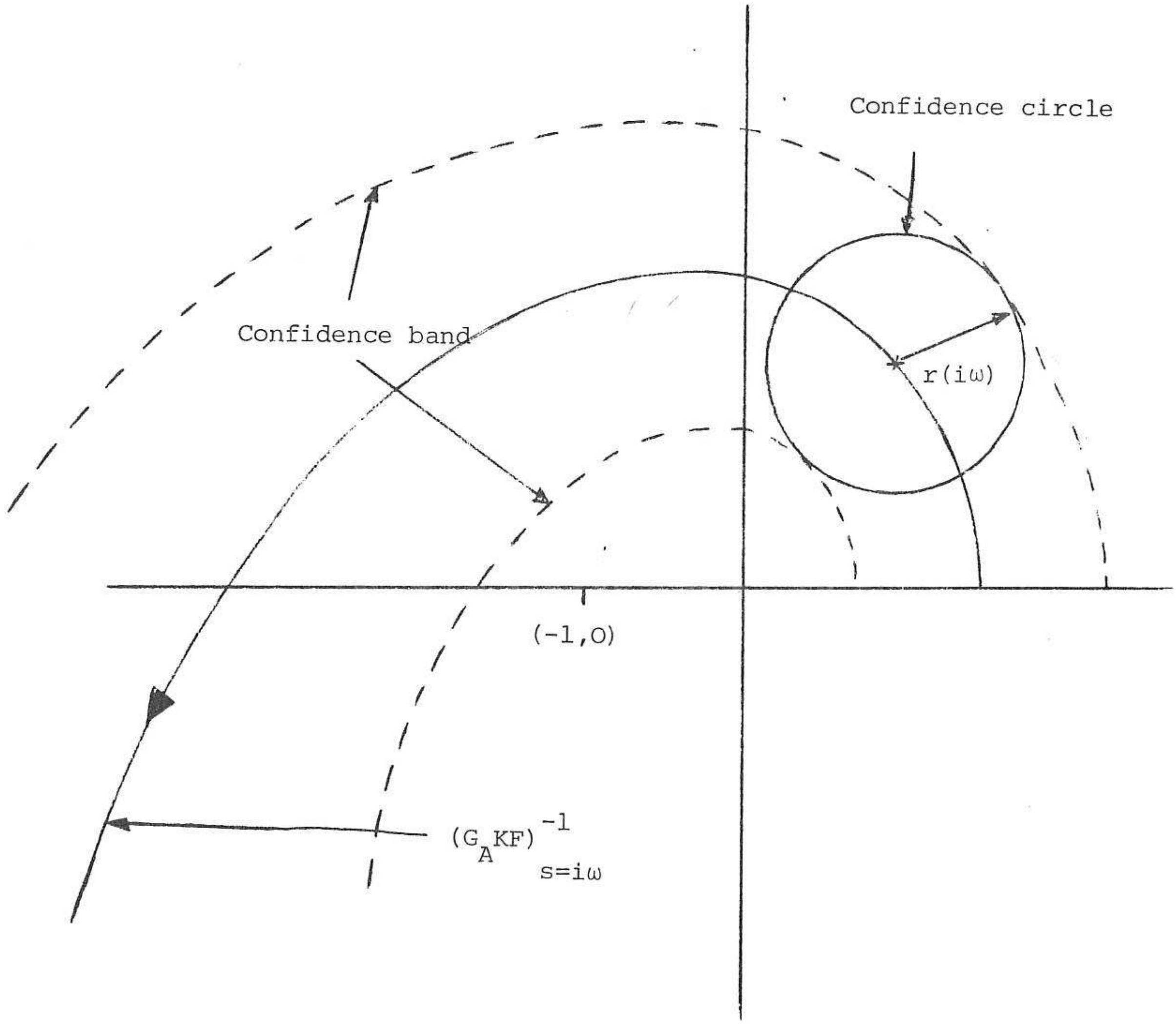

Fig. 3 Confidence band and Confidence circle

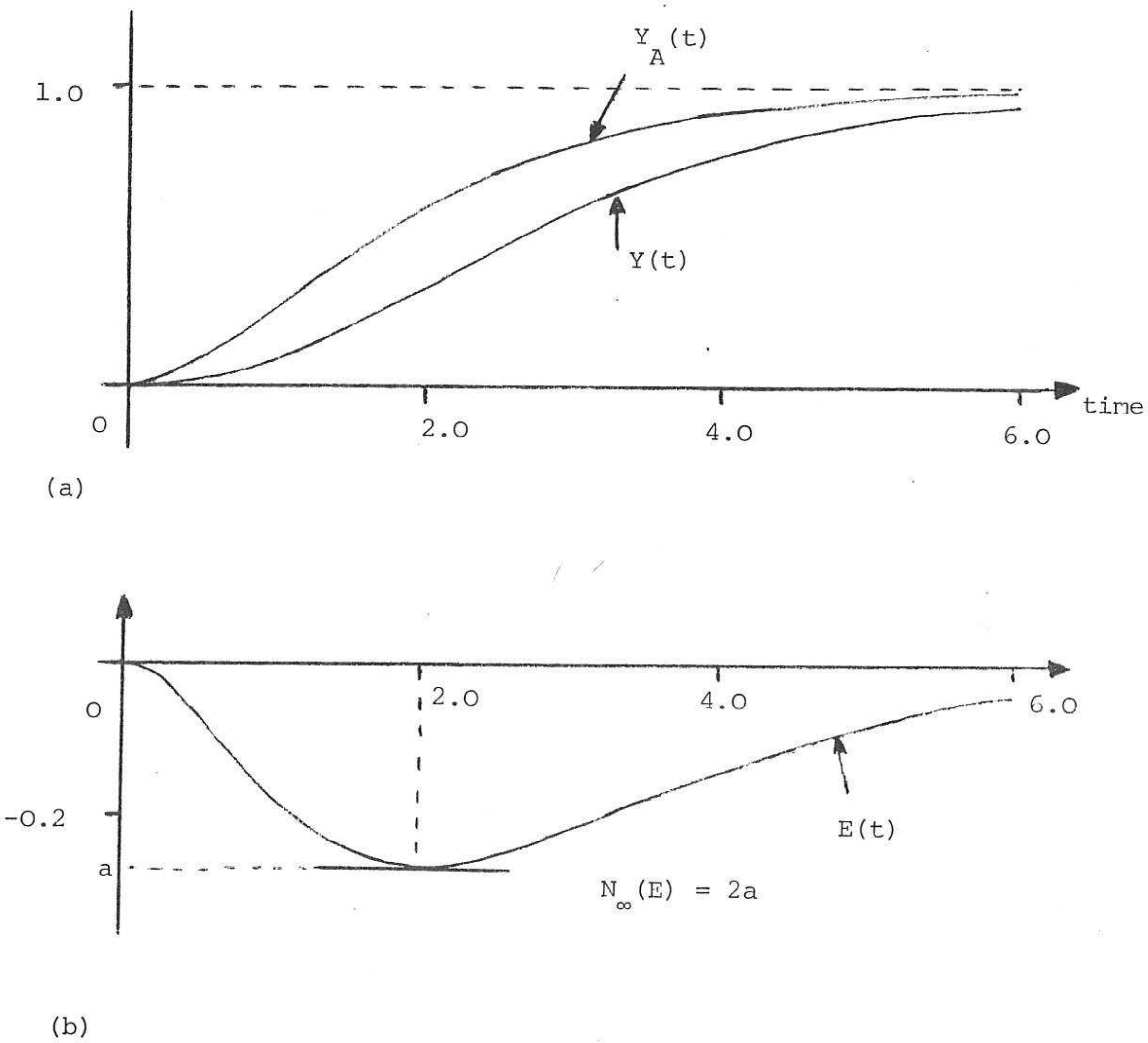

Fig. 4

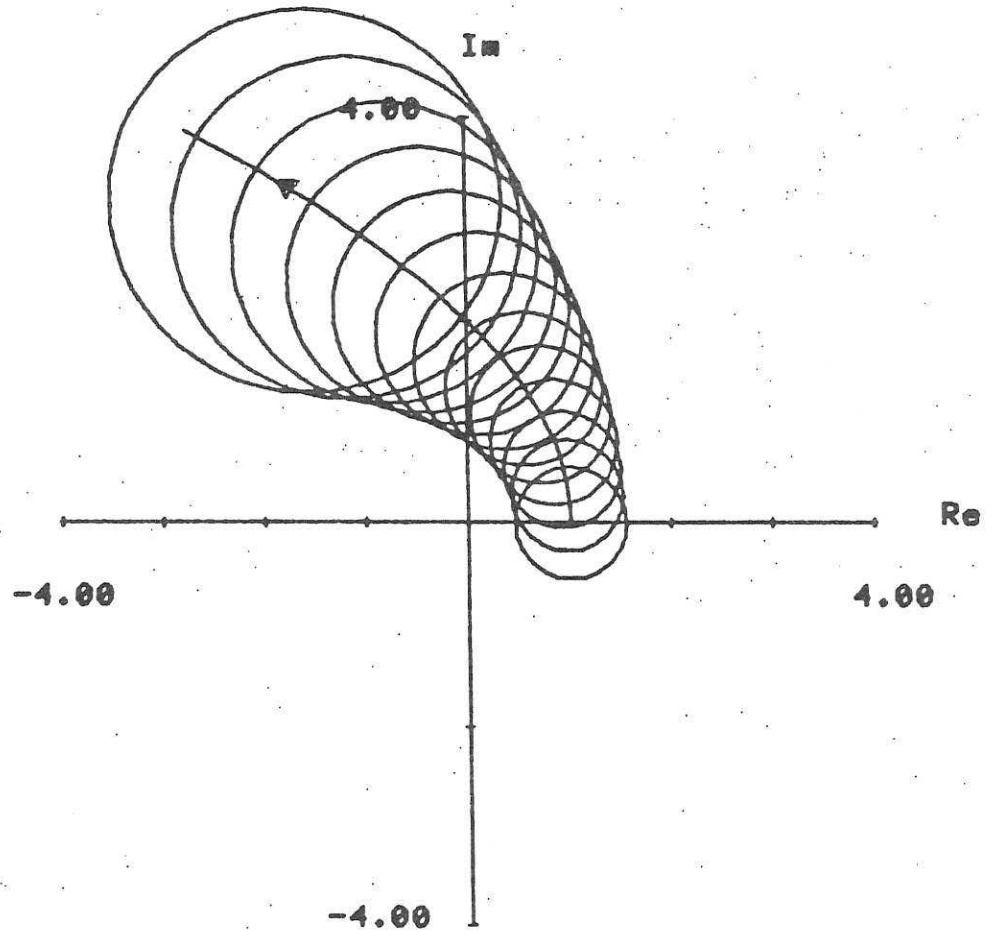

Fig. 5 Confidence Band for example 2.5 with Proportional control

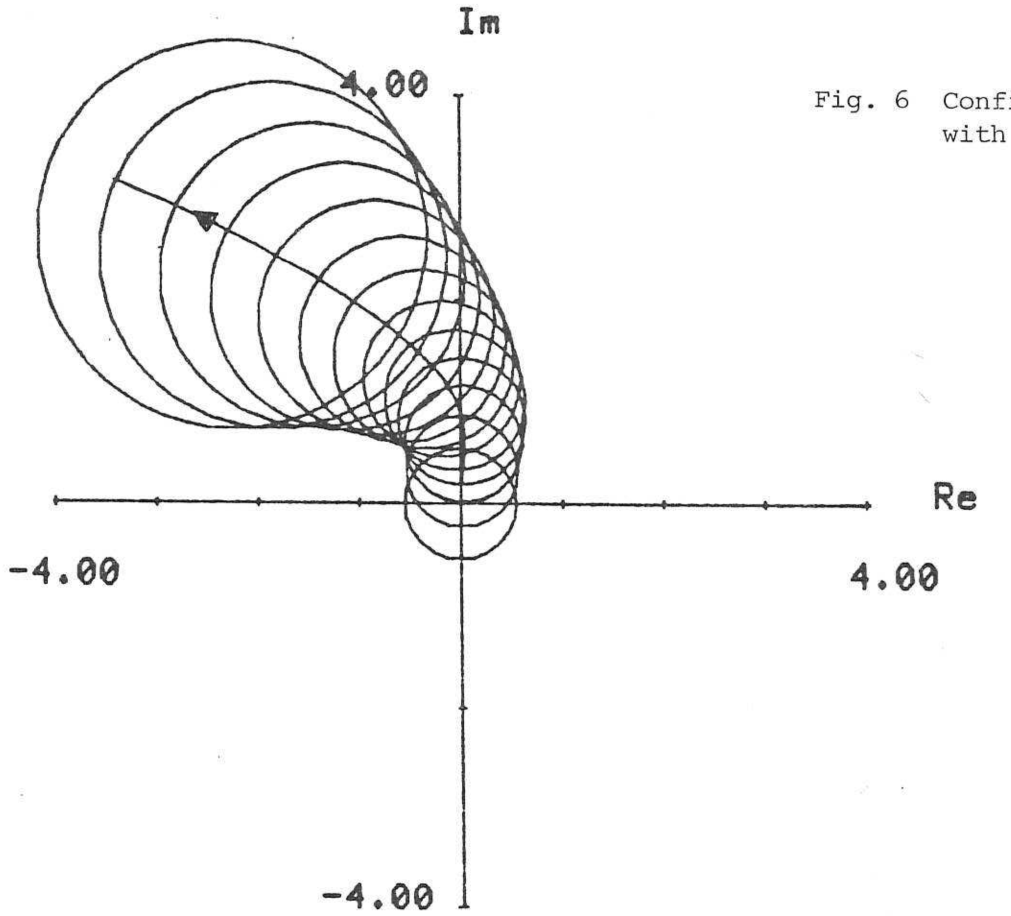

Fig. 6 Confidence Band for example 2.5
with Proportional plus Integral control

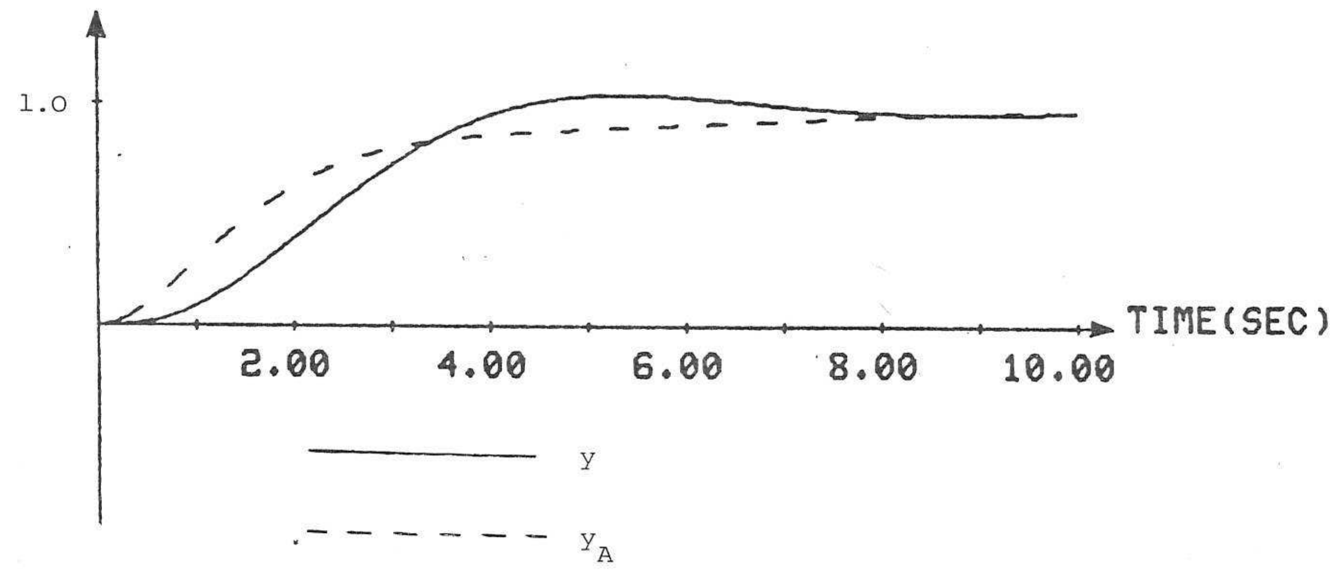

Fig. 7 Closed-loop response for example 2.5

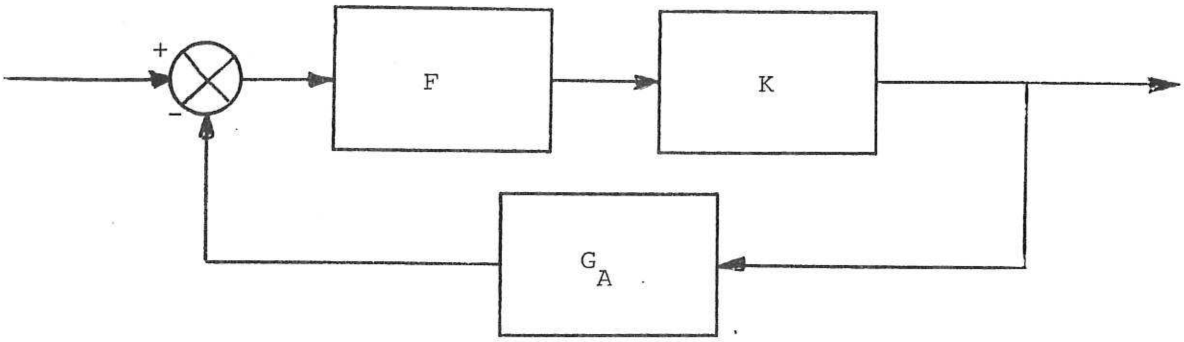

(a)

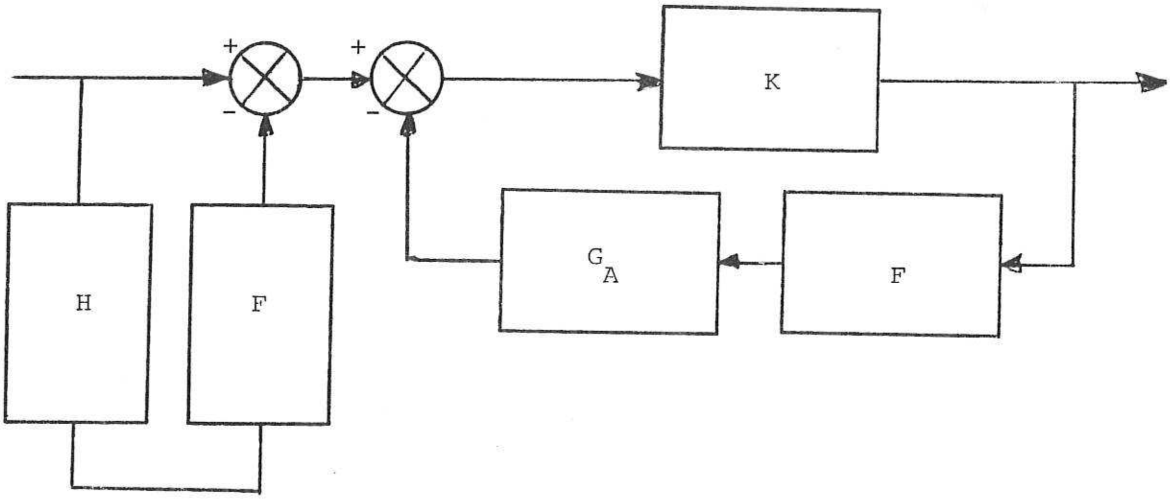

(b)

Fig. 8

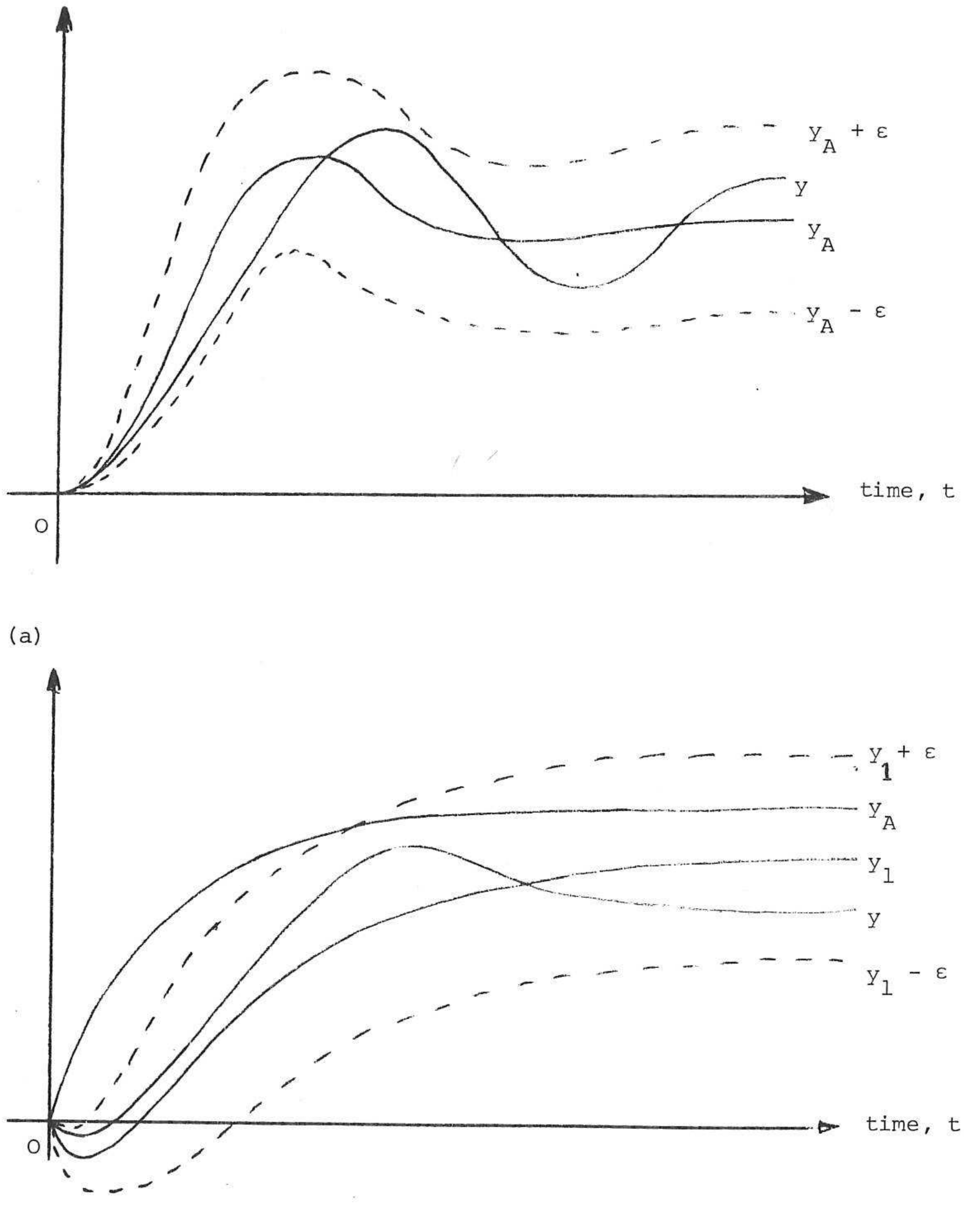

Fig. 9

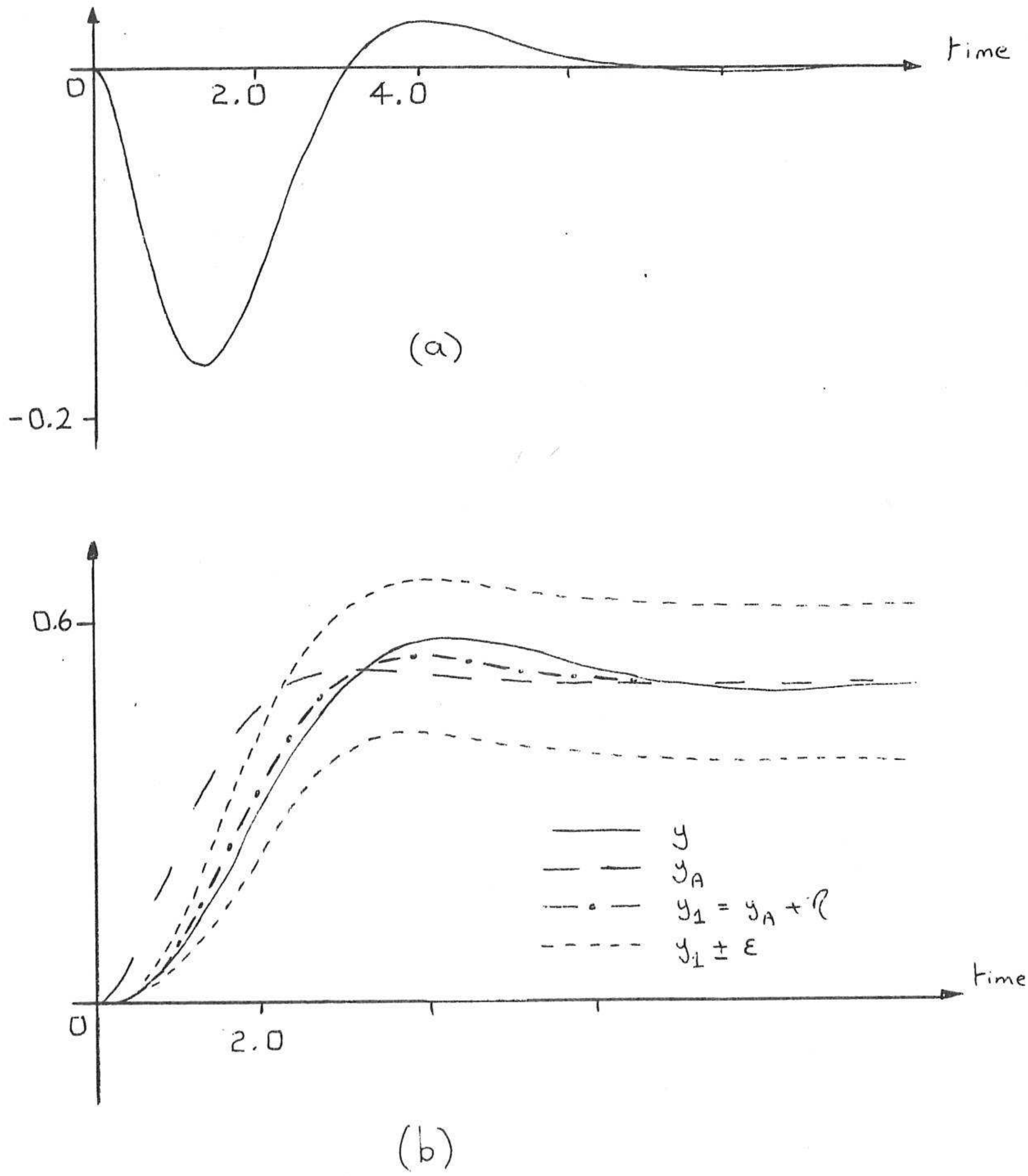

Fig 10.